

1 **A $\delta^2\text{H}$ offset correction method for quantifying root water uptake of**
2 **riparian trees**

3

4 Revised manuscript submitted to *Journal of Hydrology* (HYDROL38311)

5

6 Yue Li^{a, c}, Ying Ma^{a, c, *}, Xianfang Song^{a, c}, Lixin Wang^b, Dongmei Han^{a, c}

7

8 ^a *Key Laboratory of Water Cycle and Related Land Surface Processes, Institute of Geographic*

9 *Sciences and Natural Resources Research, Chinese Academy of Sciences, Beijing 100101,*

10 *China*

11 ^b *Department of Earth Sciences, Indiana University-Purdue University Indianapolis (IUPUI),*

12 *Indianapolis, IN 46202, United States*

13 ^c *University of Chinese Academy of Sciences, Beijing 100049, China*

14

15 ^{*} *Corresponding author,*

16 Tel.: +86 10 64880562

17 E-mail address: maying@igsnr.ac.cn

18

This is the author's manuscript of the article published in final edited form as:

Li, Y., Ma, Y., Song, X., Wang, L., & Han, D. (2021). A $\delta^2\text{H}$ offset correction method for quantifying root water uptake of riparian trees. *Journal of Hydrology*, 593, 125811. <https://doi.org/10.1016/j.jhydrol.2020.125811>

19 **Abstract**

20 Root water uptake plays an important role in water cycle in
21 Groundwater-Soil-Plant-Atmosphere-Continuum. Stable isotopes ($\delta^2\text{H}$ and $\delta^{18}\text{O}$) are effective
22 tools to quantify the use of different water sources by plant roots. However, the widespread
23 $\delta^2\text{H}$ offsets of stem water from its potential sources due to $\delta^2\text{H}$ fractionation during root water
24 uptake result in conflicting interpretations of water utilization using stable isotopes. In this
25 study, a potential water source line (PWL), i.e., a linear regression line between $\delta^{18}\text{O}$ and $\delta^2\text{H}$
26 data of both soil water at different depths and groundwater, was proposed to correct $\delta^2\text{H}$
27 offsets of stem water. The PWL-corrected $\delta^2\text{H}$ was determined by subtracting the deviation
28 between $\delta^2\text{H}$ in stem water and PWL from the original value. The MixSIAR model coupled
29 with seven types of input data (i.e. various combinations of single or dual isotopes with
30 uncorrected or corrected $\delta^2\text{H}$ data by PWL or soil water line (SWL)) were used to determine
31 seasonal variations in water uptake patterns of riparian tree of *Salix babylonica* (L.) along the
32 Jian and Chaobai River in Beijing, China. These methods were evaluated via three criteria
33 including Akaike Information Criterion (AIC), Bayesian Information Criterion (BIC) and root
34 mean square error (RMSE). Results showed that different types of input data led to
35 considerable differences in the contributions of soil water at upper 30 cm (9.9–57.6%) and
36 below 80 cm depths (29.0–76.4%). Seasonal water uptake patterns were significantly different
37 especially when $\delta^2\text{H}$ offset was pronounced ($p < 0.05$). The dual-isotopes method with
38 uncorrected $\delta^2\text{H}$ underestimated the contributions of soil water in the 0–30 cm layer (by 30.4%)
39 and groundwater (by 56.3%) compared to that with PWL-corrected $\delta^2\text{H}$. The PWL correction
40 method obtained a higher groundwater contribution (mean of 29.5%) than that estimated by the
41 SWL correction method (mean of 24.5%). The MixSIAR model using dual-isotopes with
42 PWL-corrected $\delta^2\text{H}$ produced the smallest AIC (94.1), BIC (91.9) and RMSE values (4.8%)
43 than other methods (94.9–101.7, 92.6–99.5 and 5.3–12.4%, respectively), which underlined

44 the best performance of PWL correction method. The present study provides crucial insights
45 into quantifying accurate root water uptake sources even if $\delta^2\text{H}$ offset exists.

46 **Key words:** Root water uptake; $\delta^2\text{H}$ offset; MixSIAR model; Potential water source line;
47 Riparian tree

48

49 **1. Introduction**

50 Terrestrial vegetation plays an irreplaceable role in the global water cycle because 65% of
51 precipitation was transported from land surfaces to the atmosphere by means of plant
52 transpiration (Wang et al., 2014; Good et al., 2015; Wei et al., 2017). In recent years, a
53 growing number of studies have focused on the water cycle in
54 Groundwater-Soil-Plant-Atmosphere-Continuum (GSPAC), which is mainly controlled by
55 plant transpiration (Gou and Miller, 2014; Jiao et al., 2019). In particular, root water uptake is
56 one of the most important components in GSPAC by indicating the plants' abilities to take up
57 different water sources and respond to variable hydrological conditions (Ma and Song, 2016;
58 Barbeta et al., 2019). However, the explicit quantification of root water uptake remains
59 challenging due to the complexity and variability of plant water use.

60 Stable isotope tracing technique, as an efficient tool with minimum damage to plants
61 during sampling, has been widely used in exploring root water uptake by comparing isotopic
62 compositions of stem water and its potential water sources (Dawson and Ehleringer, 1991;
63 Asbjornsen et al., 2007; Yang et al., 2015a; Ma and Song, 2016; Rothfuss and Javaux, 2017;
64 Yang et al., 2018). The quantification of the main plant water sources is usually carried out
65 via the statistically-based multisource mixing models such as the IsoSource model and
66 Bayesian mixing models (e.g., SIAR, MixSIR and MixSIAR) (Rothfuss and Javaux, 2017;
67 Wang et al., 2019a). Specifically, MixSIAR not only accounts for the uncertainties in the root
68 water uptake estimations of isotope ratios of stem water and its corresponding water sources,

69 but also provides an optimal solution rather than a range of feasible solutions (Rothfuss and
70 Javaux, 2017; Wang et al., 2019a). The isotopic tracing method relies on a basic assumption
71 that no isotopic fractionation occurs during root water uptake (Dawson and Ehleringer, 1991;
72 Ehleringer and Dawson, 1992). Hydrogen ($\delta^2\text{H}$) and oxygen ($\delta^{18}\text{O}$) isotopes of twig/xylem
73 water represents a weighted mean signature of all water sources used by plants respectively to
74 their contributions (Dawson and Ehleringer, 1993; Ehleringer and Dawson, 1992). Both $\delta^2\text{H}$
75 and $\delta^{18}\text{O}$ isotopes of stem water should match those of source water if the assumption of no
76 isotopic fractionation is true (Lin and Sternberg, 1993; Barbeta et al., 2019).

77 However, some studies reported that $\delta^2\text{H}$ fractionation occurred in root water uptake for
78 some halophytes and xerophytes species (Lin and Sternberg, 1993; Ellsworth and Williams,
79 2007). As a result, the $\delta^2\text{H}$ of stem water was far less than that of soil water, groundwater, and
80 river water, which were possible sources of the root water uptake. Lin and Sternberg (1993)
81 found that the depletion of $\delta^2\text{H}$ in stem water ranged from 2–13‰ compared to that of source
82 water both in the field and greenhouse experiments for coastal wetland plants. It was reported
83 that 3–9‰ depletion in $\delta^2\text{H}$ of stem water in comparison to that of soil water was observed in
84 twelve of sixteen shrubs and tree species from arid and semi-arid regions in greenhouse
85 experiments by Ellsworth and Williams (2007). These $\delta^2\text{H}$ offsets of stem water from their
86 potential sources due to isotopic fractionation challenged the reliability of isotopic tracing
87 method in identifications of plant water sources (Barbeta et al., 2019). A growing number of
88 studies showed that $\delta^2\text{H}$ offsets of stem water also existed in non-halophytes and
89 non-xerophytes such as the riparian trees (Brooks et al., 2010; Zhao et al., 2016; Geris et al.,
90 2017; Barbeta et al., 2019) and the laboratory-controlled tree species (Vargas et al., 2017;
91 Barbeta et al., 2020). These $\delta^2\text{H}$ offsets of stem water mainly resulted from $\delta^2\text{H}$ fractionation
92 occurring in roots or between stem and root water, which was related to soil water loss, soil
93 type as well as leaf transpiration (Lin and Sternberg, 1993; Vargas et al., 2017; Barbeta et al.,

94 2019). Therefore, the $\delta^2\text{H}$ offsets caused by hydrogen fractionation should be kept in mind in
95 applications such as quantifying sources of root water uptake.

96 Previous studies usually did not take the $\delta^2\text{H}$ offsets of stem water into account and still
97 used single or dual-isotopes with uncorrected $\delta^2\text{H}$ method to quantify plant water sources.
98 They usually speculated that a missing water source in the sampling process led to the $\delta^2\text{H}$
99 offsets (Bowling et al., 2017). Evaristo et al. (2017) indicated that plant water source
100 estimations were less sensitive to $\delta^2\text{H}$ fractionation when both $\delta^2\text{H}$ and $\delta^{18}\text{O}$ were combined
101 within a Bayesian inference approach. On the contrary, some studies confirmed that there
102 were remarkably divergent source water contributions either using single uncorrected $\delta^2\text{H}$,
103 single $\delta^{18}\text{O}$ or both isotopes due to $\delta^2\text{H}$ offsets (Barbeta et al., 2019; Barbeta et al., 2020). In
104 order to avoid inaccurate results caused by pronounced $\delta^2\text{H}$ offsets, some studies directly
105 used single $\delta^{18}\text{O}$ to quantify plant water sources (Asbjornsen et al., 2007; Goebel et al., 2015).
106 Nevertheless, single isotopic tracer is insufficient to identify plant water sources when the
107 isotopic composition of stem water matches with several water sources (Barbeta et al., 2019;
108 Parnell et al., 2010). Therefore, neither single nor dual-isotopes method using uncorrected
109 isotopes is effective for the identification of plant water sources when $\delta^2\text{H}$ offsets exist. How
110 to correct $\delta^2\text{H}$ offsets and make accurate estimations of plant water sources is an urgent need.

111 A concept of line-condition excess (lc-excess) which was originally used to describe the
112 $\delta^2\text{H}$ offset of the river water from the local meteoric water line (LMWL) was presented by
113 Landwehr and Coplen (2006). Recently, Barbeta et al. (2019) modified the lc-excess and
114 corrected $\delta^2\text{H}$ of stem water for riparian trees by subtracting the SW-excess, which represents
115 for the $\delta^2\text{H}$ offsets of stem water from their corresponding soil water line (SWL). The SWL
116 correction method only considered soil water as potential water sources for plants. However,
117 the potential water sources also include other sources such as groundwater, rock moisture, fog
118 water, and dew water (Evaristo et al., 2015; Wang et al., 2017a; Wang et al., 2019b). In

119 particular, groundwater serves as an important and independent water source for
120 phreatophytes especially during drought periods or in arid and semiarid regions (Contreras et
121 al., 2011; Miguez-Macho and Fan, 2012; Fan, 2015), Mediterranean region (Dawson and Pate,
122 1996), and even humid region (Vincke and Thiry, 2008). Several tree species could tap into
123 capillary fringe or even water tables to take up groundwater directly to meet transpiration
124 needs (Song et al., 2016; Christina et al., 2018). Groundwater is extracted by trees more
125 efficiently than soil water in the unsaturated zone because a few deep roots can withdraw a
126 large quantities of groundwater (20%) for transpiration (Ferro et al., 2003). Although
127 groundwater is identified as an important water source, it was not considered in the SWL
128 correction method due to its similar isotopic values with deep soil water in Barbeta et al.
129 (2019). However, the isotopic composition of groundwater may vary greatly from that in the
130 deep soil water. Therefore, the $\delta^2\text{H}$ offset correction should consider the isotopic values of
131 potential water sources such as soil water at different depths and groundwater if the plants
132 have deep roots to acquire groundwater.

133 In this study, the MixSIAR model accompanied with a developed $\delta^2\text{H}$ offset correction
134 method was used to quantify root water uptake patterns of riparian trees along the Jian and
135 Chaobai River in Beijing, China. The objectives of this study were to: (1) propose a water
136 source line that can correct the $\delta^2\text{H}$ offset of stem water from its potential water sources; (2)
137 compare the outputs of MixSIAR model using single or dual-isotopes method with
138 uncorrected or corrected $\delta^2\text{H}$ input data; (3) evaluate the effects of $\delta^2\text{H}$ offsets and single or
139 dual-isotopes method on determination of water sources for riparian trees.

140 **2. Materials and methods**

141 *2.1. Theoretical consideration*

142 *2.1.1. PWL definition*

143 The potential water source line (PWL) was presented to correct the $\delta^2\text{H}$ offset of stem

144 water from the potential water sources including both soil water at different depths and
145 groundwater. $\delta^2\text{H}$ values of stem water corrected by PWL can match those of source water.
146 The PWL was proposed on the basis of the concept of lc-excess, which was defined by
147 Landwehr and Coplen (2006) as following:

$$148 \quad \text{lc-excess} = \delta^2\text{H} - a\delta^{18}\text{O} - b, \quad (1)$$

149 where a and b represent the slope and intercept of LMWL. $\delta^2\text{H}$ and $\delta^{18}\text{O}$ in Eq. (1) are isotopic
150 compositions of river water samples.

151 Generally, trees cannot take up rainwater or river water directly but rely on soil water. In
152 order to access the $\delta^2\text{H}$ deviation of stem water from the SWL (i.e., SW-excess), Barbeta et al.
153 (2019) changed the above lc-excess formula into:

$$154 \quad \text{SW-excess} = \delta^2\text{H} - a_s\delta^{18}\text{O} - b_s, \quad (2)$$

155 where a_s and b_s represent the slope and intercept of SWL, respectively. $\delta^2\text{H}$ and $\delta^{18}\text{O}$ in Eq. (2)
156 are isotopic compositions of stem water. The SW-excess indicates the $\delta^2\text{H}$ offsets of stem
157 water with respect to their corresponding SWL which limits the plant water sources to only soil
158 water pools. Positive SW-excess value means that the $\delta^2\text{H}$ in stem water is more enriched
159 than the SWL, while negative value means that $\delta^2\text{H}$ in stem water is more depleted than SWL.
160 The concept of the SWL correction method is shown in Fig. 1.

161 Besides soil water, groundwater is a crucial water source especially for phreatophytes
162 growing in areas with shallow water table depth (WTD). Groundwater and deep soil water
163 cannot be merged into one source for the estimations of water uptake patterns, when their
164 isotopic compositions are significantly different. Groundwater will greatly affect the fitting of
165 the correction water line. Therefore, the PWL was proposed by performing a linear regression
166 on all soil water and groundwater isotope data, as shown in Fig. 1. The $\delta^2\text{H}$ deviation of stem
167 water from the PWL (i.e., PW-excess) was as follows:

$$168 \quad \text{PW-excess} = \delta^2\text{H} - a_p\delta^{18}\text{O} - b_p, \quad (3)$$

169 where a_p and b_p are the slope and intercept of the PWL, respectively.

170 Positive value of PW-excess means that the $\delta^2\text{H}$ in stem water is more enriched than the
171 PWL. The larger the positive value is, the greater the degree of isotopic enrichment is. On the
172 contrary, negative value of PW-excess represents that $\delta^2\text{H}$ in stem water is more depleted than
173 that the PWL. The larger the negative value is, the greater the degree of isotopic depletion is.
174 When PW-excess is zero, there is no $\delta^2\text{H}$ offset between stem water and the PWL. The $\delta^2\text{H}$
175 value of stem water is corrected by subtracting the corresponding PW-excess from the original
176 value.

177 <Figure 1>

178 2.1.2. *MixSIAR model and different types of input data*

179 The MixSIAR model (v3.1) incorporating with stable isotopes ($\delta^2\text{H}$ and $\delta^{18}\text{O}$) was used to
180 calculate contributions of potential water sources to plant stem water. The isotopic values of
181 stem water were referred as the mixture data, whereas those of soil water at different depths and
182 groundwater were set as the source data. The Markov chain Monte Carlo (MCMC) parameter
183 run length in the MixSIAR model was selected as “very long” for convergence. The model
184 errors were evaluated via the process and residual errors. The calculated 50% percentile of the
185 posterior contribution was referred as the main proportional contribution of each water source
186 to stem water in this study (Stock and Semmens, 2013). More details about MixSIAR model
187 (v3.1) could be found in Stock and Semmens (2013).

188 In order to evaluate the effects of $\delta^2\text{H}$ offset in stem water and single or dual-isotopes
189 method on quantifying root water uptake, we compared the performance of MixSIAR model
190 input with seven types of isotopic data for stem water including (1) uncorrected $\delta^2\text{H}$ and $\delta^{18}\text{O}$,
191 (2) single uncorrected $\delta^2\text{H}$, (3) single $\delta^{18}\text{O}$, (4) dual isotopes with $\delta^2\text{H}$ corrected by the SWL
192 (subtracting the SW-excess from the $\delta^2\text{H}$ values) and $\delta^{18}\text{O}$, (5) single $\delta^2\text{H}$ corrected by the

193 SWL, (6) dual isotopes with $\delta^2\text{H}$ corrected by the PWL (subtracting the PW-excess from the
194 $\delta^2\text{H}$ values) and $\delta^{18}\text{O}$, and (7) single $\delta^2\text{H}$ corrected by the PWL.

195 To assess the effectiveness of the developed $\delta^2\text{H}$ offset correction method in identifying
196 root water uptake sources, two types of evaluation methods were used to evaluate the results of
197 seven types of input data. The first method was based on the correlations between plant water
198 source estimations and environment variables. Previous studies showed that $\delta^2\text{H}$ offsets and
199 root water uptake patterns were affected by different environmental variables such as vapor
200 pressure deficit (VPD), precipitation, soil sand content (SSC), WTD and soil water content
201 (SWC) (Qian et al., 2017; Vargas et al., 2017; Wang et al., 2017b; Barbeta et al., 2019). For
202 example, precipitation, the fluctuation of WTD and SWC could affect water availabilities of
203 potential water sources for trees (Qian et al., 2017). Geris et al. (2017) concluded that soil type
204 might have a strong effect on water uptake patterns. This could be explained by the fact that
205 soil types affected both precipitation infiltration and groundwater capillary rise through
206 changing soil moisture and root distribution (Vereecken et al., 2015; Zipper et al., 2015). The
207 VPD could impact the transpiration rate of plants, which was the driving force of root water
208 uptake. A significant relationship was found between the VPD and water source contributions
209 (Barbeta et al., 2019). Therefore, the correlations between plant water source estimations and
210 these multiple environment variables could be considered to evaluate the performances of
211 MixSIAR model with seven types of input data. The stronger the correlation was, the water
212 source contributions calculated by MixSIAR model were closer to actual values. The
213 correlation analysis was conducted using general linear mixed models (GLMM) in the SPSS
214 software (22.0 version) to avoid the influence of random errors (e.g., different sites and
215 sampling campaigns). The Akaike Information Criterion (AIC) and Bayesian Information
216 Criterion (BIC) values (Rascher et al., 2004) were used to compare the correlations of plant

217 water source estimations with different environmental variables among the seven types of
218 input data. The input data with the lower values of AIC and BIC were the preferred type.

219 Secondly, the deviation of water source contributions estimated with each type of input
220 data from the average values of all seven types of input data was assessed. It could reflect the
221 uncertainties of MixSIAR estimations with different input data by the root mean square error
222 (RMSE):

$$223 \quad \text{RMSE} = \sqrt{\left[\frac{1}{n} \sum_{i=1}^n (p_i - \bar{p})^2 \right]}, \quad (4)$$

224 where n indicates the number of all water sources including soil water at different depths and
225 groundwater at all sites and dates, p_i is the proportional contribution of the i th water source
226 estimated by MixSIAR model with one certain type of input data, and \bar{p} is the average
227 contribution of the i th water source calculated through seven types of input data. The smaller
228 the RMSE value is, the smaller the uncertainties of plant water source estimations are. The best
229 type of input data for quantification of plant water source contributions using the MixSIAR
230 model was then selected through the smallest AIC, BIC and RMSE values.

231 2.2. Field observations

232 2.2.1. Study area and field measurements

233 In order to test the correction method of stem water $\delta^2\text{H}$ offset by PWL for determining
234 plant water sources, experiments for riparian trees of *S. babylonica* were conducted during
235 April to November in 2019 along the reaches of the Jian and Chaobai River in Shunyi district,
236 Beijing, China (40°07'30"N, 116°40'37"E) (Fig. 2). The study area has a temperate continental
237 sub-humid monsoon climate. The annual average temperature is 11.5 °C and annual average
238 evaporation is 1175 mm. The annual average precipitation is 610 mm, with 80% of which
239 occurring in the wet season from June to August. The water depth in river is mean of 1.4 m in
240 the reach of Jian River with a width of 50–90 m, and remains approximately 0.7 m in the reach

241 of the Chaobai River with a width of about 200 m. *S. babylonica* is one of the most widely
242 distributed riparian trees with growing season starting from late April to early November. With
243 a rooting system suitable for waterlogging (approximately 4 m deep), *S. babylonica* can
244 survive being below the water tables (Markus-Michalczyk et al., 2019; Martorello et al., 2020).

245 <Figure 2>

246 Three representative sites in the riparian zone alongside the Jian River (site A) and Chaobai
247 River (sites B and C) with different soil textures and WTDs were selected in this study area
248 (Fig. 2). The soil textures within 0–3 m depth were mainly clay loam, sandy loam, and sand for
249 sites A, B, and C, respectively (Table 1). There was extremely significant difference in the
250 SSC ($p < 0.001$) among sites A (33.4%), B (80.6%) and C (90.8%). The annual mean WTD
251 was significantly different among sites A (21.1 m), B (2.3 m) and C (1.6 m). Both soil water
252 and groundwater can be taken up by *S. babylonica* easily at sites B and C due to shallow WTD.
253 They were used to compare the performances of MixSIAR model with $\delta^2\text{H}$ corrected by the
254 PWL and SWL. The site A was selected as a comparison where the potential water sources
255 for *S. babylonica* were only confined to the soil water sources at different depths under the
256 deep WTD, and the PWL was the same as SWL. These three sites with various environmental
257 conditions were adequate to qualitatively evaluate the significance of the PWL correction
258 method for quantifying root water uptake sources of riparian trees and evaluate the
259 performance of MixSIAR model with seven types of input data.

260 <Table 1>

261 Daily meteorological data including temperature, radiation and relative humidity was
262 collected from the meteorological observation station (ET007, Insentec instrument, Hangzhou,
263 China) in this study area (Fig. 2). Daily VPD was estimated through relative humidity and
264 temperature. The daily precipitation data was recorded via a tilting rain gauge (SL3-1,
265 Shanghai meteorological instrument, Shanghai, China) installed on the opposite side of site C.

266 The WTD was measured once a month from the groundwater monitoring wells constructed at
267 each site.

268 2.2.2. *Water sampling and isotope analysis*

269 Water samples of precipitation, river, groundwater, stem, and soil were collected for $\delta^2\text{H}$
270 and $\delta^{18}\text{O}$ analysis. Precipitation greater than 1.5 mm was collected during the observation
271 period in 2019. The polyethylene bottle coupled with a funnel and plastic ball was used to
272 avoid evaporation (Yang et al., 2015b). Water samples of river, groundwater, stem, and soil
273 were collected on the same day with six campaigns on May 5, June 14, July 26, August 15,
274 September 26, and November 5 in 2019. River water was sampled at a depth of 0.3 m below the
275 water surface using the organic glass hydrophore. Groundwater was sampled from the
276 monitoring well at each site by a water pump.

277 *S. babylonica* trees in three plots with distances of 5, 10, and 20 m away from the river
278 bank at each site were selected for stem water isotope analysis (Fig. 2). The mean diameter at
279 breast height and average height of the studied trees were 66.5 cm and 8.0 m, respectively.
280 Three non-green and suberized stems approximately 10 mm in diameter were taken from twigs
281 of each tree and combined to represent a single stem sample. They were removed the bark and
282 phloem tissue, immediately placed into air-tight glass vials and sealed with parafilm.

283 Soil samples were collected within 1 m of each tree using a power auger with the petrol
284 engine-driven post driver (CHPD78, Christie Engineering Company, Sydney, Australia). Soil
285 was sampled at depths of 5, 10, 15, 20, 30, 40, 60, 80, 100, 150, 200, 250, and 300 cm. The
286 roots were removed, and then soil samples were placed into air-tight glass vials and sealed with
287 parafilm. The soil samples were also used for gravimetric SWC measurements by oven-dry
288 method and soil texture measurements by a laser particle size analyzer (Mastersize-2000,
289 Malven Instruments Ltd., UK).

290 All soil and stem samples were kept frozen in a refrigerator until water extraction. The
291 water contained in the stem and soil samples were collected using an automatic cryogenic
292 vacuum distillation system (LI-2100, LICA, Beijing, China). The extraction progress was
293 described in detail by Wu et al. (2019a). All the water extractions were completed, which had
294 been checked by oven drying samples at 105 °C for 12 h and reweighing them, to ensure
295 complete extraction (Yang et al., 2015b).

296 The isotopic compositions of rainwater, soil water, groundwater, and river water were
297 measured by an isotopic ratio infrared spectroscopy (IRIS) system (DLT-100, Los Gatos
298 Research, mountain view, USA). The measurement precision of the IRIS system was $\pm 1\%$ for
299 $\delta^2\text{H}$ and $\pm 0.1\%$ for $\delta^{18}\text{O}$ (Wang et al., 2009). Because organic contaminants in the water
300 cryogenically extracted from the tree stems would affect the isotopic measurements by the
301 IRIS method (Zhao et al., 2011), we used an Isotope Ratio Mass Spectrometry (IRMS) system
302 (MAT253, Thermo Fisher Scientific, Bremen, Germany) to measure the $\delta^2\text{H}$ and $\delta^{18}\text{O}$ in stem
303 water. The precision of the IRMS system was $\pm 1\%$ for $\delta^2\text{H}$ and $\pm 0.1\%$ for $\delta^{18}\text{O}$, respectively.
304 The measured isotopic compositions for different waters were calibrated and normalized
305 against the Vienna Standard Mean Ocean Water (VSMOW). No significant difference in $\delta^2\text{H}$
306 ($p = 0.98$) and $\delta^{18}\text{O}$ ($p = 0.89$) measurements for groundwater, rainwater and soil water was
307 observed between the IRIS and IRMS methods.

308 There was no significant difference in water isotopes among the trees in the three plots at
309 each site, and they were considered as three replicates to analyze the water sources of riparian
310 trees. Four soil layers (0–30, 30–80, 80–150, 150–300 cm) were divided based on seasonal
311 variations in SWC and soil water isotopic composition at different depths. The isotopic ratios
312 of stem water and soil water in each layer were input into MixSIAR model to quantify the
313 water source contributions for riparian trees in each plot, and then the estimated results of
314 three plots were averaged to determine the root water uptake patterns at each site.

315 2.3. Statistical analysis

316 One-way analysis of variance (ANOVA) with Kolmogorov-Smirnov, Levene's and
317 post-hoc Tukey's tests ($p < 0.05$) were used to examine differences in the isotopic
318 compositions of different water sources as well as differences in the $\delta^2\text{H}$ offsets among three
319 sites. Two-way ANOVA was performed to detect the significant effects of both sampling sites
320 and dates on the $\delta^2\text{H}$ offsets and the differences of proportional contributions of water sources
321 among seven types of input data. The above statistical analysis was performed in the SPSS
322 software (22.0, Inc., Chicago, IL, USA).

323 3. Results

324 3.1. Environmental variables

325 The total precipitation was 399 mm during the observation period in 2019 (Fig. 3). There
326 were pronounced differences in seasonal variations of precipitation ($p < 0.01$). The
327 accumulated monthly precipitation during April to November was 18.4, 25.8, 19.5, 133.7, 89.1,
328 79.1, 32.9 and 0.6 mm, respectively. Monthly mean VPD was 0.9, 1.4, 1.4, 1.2, 1.0, 0.8, 0.5 and
329 0.3 kPa from April to November, respectively, with mean of 1.0 kPa and standard deviation
330 (SD) of 0.5 kPa (Fig. 3). The WTD was significantly different among sites A (20.5 ± 0.5 m), B
331 (1.9 ± 0.3 m), and C (1.5 ± 0.1 m) ($p < 0.05$) (Fig. 3). The increase of WTD was observed at
332 sites A (from 20.0 to 21.2 m) and B (from 1.7 to 2.5 m) during the wet season, whereas WTD
333 was relatively stable at site C.

334 The depth distribution and seasonal variation in SWC exhibited significant differences
335 among the three sites ($p < 0.05$). The average SWC in the 0–30 cm layer was larger at site A
336 (mean of 0.16 g g^{-1} and SD of 0.03 g g^{-1}) than that at site B (mean of 0.09 g g^{-1} and SD of 0.02
337 g g^{-1}) and site C (mean of 0.09 g g^{-1} and SD of 0.03 g g^{-1}) (Fig. 4). However, the SWC in the
338 80–300 cm layer was largest (mean of 0.25 g g^{-1}) at site C, following by that at site B (mean of

339 0.21 g g⁻¹) and smallest at site A (mean of 0.20 g g⁻¹) (Fig. 4). There was an evident decline of
340 SWC in the 0–150 cm layer during May to August at sites A and B, but not at site C.

341 <Figure 3>

342 <Figure 4>

343 3.2. Isotopic compositions of different water bodies

344 The isotopic values of precipitation ranged from –68.3 to –26.0‰ for δ²H and –13.9 to
345 –6.3‰ for δ¹⁸O (Fig. 5). The LMWL fitted by the isotopic compositions of precipitation was
346 established as: δ²H = 5.5δ¹⁸O –7.9 ($R^2 = 0.81$) during the observation period in 2019.

347 Groundwater gradually enriched from site A (mean of –71.1‰ for δ²H and –10.2‰ for δ¹⁸O)
348 to site B (mean of –55.7‰ for δ²H and –6.9‰ for δ¹⁸O) and site C (mean of –51.1‰ for δ²H
349 and –6.4‰ for δ¹⁸O) (Fig. 5). The isotopic compositions of groundwater were more depleted
350 than those of river water at site A ($p < 0.001$) (Fig. 5). Nevertheless, no significant difference
351 was found in seasonal variations of isotopic values between groundwater and river water at
352 sites B and C during the observation period ($p > 0.05$).

353 Soil water isotopes at different depths ranged from –86.6 to –45.6‰ for δ²H and from
354 –14.1 to –3.2‰ for δ¹⁸O at the three sites (Fig. 5). They were enriched in the 0–30 cm soil
355 layer but depleted with depth within the 0–300 cm profile at site A. It was evident that soil
356 water isotopes in the 150–300 cm layer at sites B and C were evidently affected by
357 groundwater, being more enriched than those in the 80–150 cm layer (Fig. 5).

358 The δ²H in stem water was more depleted than that of potential water sources and fell to the
359 lower right of the PWL at sites B and C in the dual-isotopes plots (Fig. 5). Nevertheless, the
360 δ¹⁸O in stem water was always within the range of that in groundwater and soil water,
361 suggesting that groundwater was an important water source for riparian trees at sites B and C.
362 As river water and groundwater interacted closely and had similar isotopic characteristics, they
363 could be pooled together as one potential water source for riparian trees at these two sites. On

364 the contrary, the $\delta^{18}\text{O}$ in stem water (mean of -7.4‰) was remarkably enriched than that of
365 groundwater (mean of -10.2‰) and more depleted than that of river water (mean of -6.9‰) at
366 site A. Trees could not take up groundwater under the deep WTD (mean of 20.5 m). Therefore,
367 neither groundwater nor river water was considered as water sources for riparian trees at site A.

368 <Figure 5>

369 3.3. $\delta^2\text{H}$ offsets of stem water

370 The PWL and SWL for sites A (PWL was the same as SWL), B and C during the
371 observation period were fitted with $R^2 > 0.66$ ($p < 0.001$) in Fig. 5. The slope of SWL and PWL
372 indicated the evaporation degree of soil water sources and potential water sources, respectively.
373 On average, the SWL had a slope of 6.4, 4.2, and 4.8 at site A, B, and C, respectively. In
374 comparison, the slopes of PWL at site B (mean of 4.5) and site C (mean of 5.3) were larger than
375 those of SWL, which indicated that the evaporation degree of potential water sources was
376 smaller than that of soil water sources. Additionally, evaporation of both soil water and
377 potential sources were strongest at site B among the three sites.

378 The $\delta^2\text{H}$ offset of stem water from its potential water sources was calculated by the
379 PW-excess and SW-excess (Fig. 6). The mean SW-excess value during the observation period
380 was -4.7 , -5.1 and -8.0‰ for site A, B, and C, respectively. The PW-excess values (mean of
381 -8.5‰) were significantly lower than SW-excess values (mean of -6.5‰) over the
382 observation period at sites B and C ($p < 0.05$). There were pronounced seasonal differences in
383 the $\delta^2\text{H}$ offset characteristics among the three sites ($p < 0.001$) (Fig. 6). The average value of
384 PW-excess (same as SW-excess) for site A remained stable with SD of 0.8‰ during the
385 observation period. The average value of PW-excess varied greatly, ranging from -13.7‰ to
386 -1.7‰ among the six sampling campaigns during the observation period at sites B and C (Fig.
387 6). Extremely significant $\delta^2\text{H}$ offset of stem water occurred on May 5, June 14, and July 26 ($p <$
388 0.01).

389 <Figure 6>

390 3.4. Comparison of water use patterns determined by different input data

391 The proportional contributions of different potential water sources to riparian trees
392 estimated by MixSIAR model with seven types of input data were shown in Fig. 7 and Table 2.
393 When using dual-isotopes method with $\delta^2\text{H}$ in stem water corrected by PWL, the average
394 contributions of soil water in the 0–30, 30–80, 80–150, 150–300 cm layers and groundwater
395 were 22.4, 18.3, 14.1, 16.7 and 28.5%, respectively (Table 2). There were significant
396 differences in proportional contributions of soil water sources below 80 cm (29.0–76.4%)
397 among seven types of input data ($p < 0.05$), especially when $\delta^2\text{H}$ offset was pronounced. For
398 example, those average contributions estimated using single uncorrected $\delta^2\text{H}$ (mean of 41.4%)
399 and dual-isotopes method with uncorrected $\delta^2\text{H}$ (mean of 36.9%) were lower than those
400 estimated by single $\delta^{18}\text{O}$ (mean of 62.2%), dual-isotopes method with SWL-corrected $\delta^2\text{H}$
401 (mean of 62.7%), and dual-isotopes method with PWL-corrected $\delta^2\text{H}$ (mean of 63.6%). The
402 differences were also observed in the contribution of groundwater among seven types of input
403 data during the whole growing season ($p < 0.05$). For instance, groundwater contributed a little
404 to trees estimated using single uncorrected $\delta^2\text{H}$ (mean of 12.9%) and dual-isotopes method
405 with uncorrected $\delta^2\text{H}$ and $\delta^{18}\text{O}$ (mean of 12.9%), whereas it contributed more using single $\delta^{18}\text{O}$
406 (mean of 27.4%), single $\delta^2\text{H}$ corrected by PWL (mean of 30.6%), and dual-isotopes with $\delta^{18}\text{O}$
407 and PWL-corrected $\delta^2\text{H}$ (mean of 29.5%) (Table 2). Additionally, the PWL correction method
408 estimated a higher contribution of groundwater (mean of 29.5%) than that (mean of 24.5%)
409 estimated by the SWL correction method (Table 2).

410 <Table 2>

411 There were significant differences in seasonal water uptake patterns for riparian trees
412 among different types of input data ($p < 0.05$) (Fig. 7 and Table 2). The results calculated by
413 dual-isotopes method with PWL-corrected $\delta^2\text{H}$ showed that riparian trees mainly used water

414 from soils below 150 cm on May 5, June 14, July 26, and August 15 with contributions greater
415 than 54.6%. Then the main water uptake depth changed to the 0–150 cm layer on September 26
416 and November 5 with the contributions more than 60.5%. However, the main water uptake
417 depth estimated by single and dual-isotopes method with uncorrected $\delta^2\text{H}$ was in the 0–150 cm
418 layer during the entire observation period, with average contribution of 72.3% (Fig. 7 and
419 Table 2). The proportional contribution of soil water in the 0–30 cm layer to stem water of
420 trees during wet season (June to August) differed greatly among seven types of input data. It
421 contributed more estimated using dual-isotopes method with PWL-corrected $\delta^2\text{H}$ (with mean
422 of 25.8%), whereas the average contributions were 18.4, 20.2 and 19.6% calculated by single
423 uncorrected $\delta^2\text{H}$, single $\delta^2\text{H}$ corrected by SWL and PWL, respectively. The absolute (from -8.6%
424 to 10.6%) and relative (from -29.9% to 64.7%) differences in the contributions of tree water
425 sources were evident on several sampling campaigns especially at sites B and C between the
426 single $\delta^{18}\text{O}$ and dual-isotopes with PWL-corrected $\delta^2\text{H}$ methods (Fig. 7 and Table S1). For
427 example, the single $\delta^{18}\text{O}$ method overestimated the contributions of soil water in the 30–80 cm
428 layer by 64.2% on Aug 15, while it underestimated groundwater contributions by 26.1% on
429 September 26 at site B relative to the dual-isotopes with PWL-corrected $\delta^2\text{H}$ method.

430 <Figure 7>

431 3.5. Best input isotope data for identifying riparian tree water sources

432 The AIC and BIC values that reflected the relationship between source contributions to
433 stem water and environmental variables for selecting the preferred input data were shown in
434 Table 3. Without consideration of the $\delta^2\text{H}$ offset, both single $\delta^2\text{H}$ and dual-isotopes methods
435 displayed the largest AIC (101.7) and BIC (101.7) (Table 3). It was worth noting that the single
436 $\delta^{18}\text{O}$ method showed lower AIC (94.9) and BIC values (92.6). On the contrary, when $\delta^2\text{H}$ in
437 stem water was corrected by PWL, dual-isotopes method produced smaller AIC (94.1) and BIC
438 (91.9) than single PWL-corrected $\delta^2\text{H}$ (AIC of 98.0 and BIC of 95.8) and single $\delta^{18}\text{O}$ (AIC of

439 94.9 and BIC of 92.6). The estimations of plant water sources with corrected isotopes displayed
440 significantly smaller AIC and BIC values than those with uncorrected isotopes ($p < 0.05$). For
441 instance, the average single corrected $\delta^2\text{H}$ produced a lower AIC (97.1) and BIC (94.9) than
442 single uncorrected $\delta^2\text{H}$ (AIC of 101.7 and BIC of 99.5). Moreover, the dual-isotopes method
443 with SWL-corrected $\delta^2\text{H}$ figured out larger AIC (97.6) and BIC (95.4) values than that with
444 PWL-corrected $\delta^2\text{H}$. This suggested that dual-isotopes method with PWL-corrected $\delta^2\text{H}$ had
445 better performance than that with SWL-corrected $\delta^2\text{H}$.

446 The RMSE values for explaining the deviation of the source contributions estimated by
447 one type of input data from the average source contributions of different input data were shown
448 in Table 3. RMSE value was remarkably smaller when using dual-isotopes than that using
449 single isotope ($p < 0.05$) (Table 3), whether $\delta^2\text{H}$ offset was corrected or not. For example,
450 RMSE value was 12.4% when using single uncorrected $\delta^2\text{H}$, whereas it was 9.5% when using
451 dual-isotopes method with uncorrected $\delta^2\text{H}$. The water source contribution estimations with
452 corrected isotopes displayed significantly smaller RMSE values (mean of 5.1%) than those
453 with uncorrected isotopes (mean of 9.6%) ($p < 0.05$). Furthermore, the dual-isotopes method
454 with SWL-corrected $\delta^2\text{H}$ had significant higher RMSE values than the dual-isotopes method
455 with PWL-corrected $\delta^2\text{H}$ ($p < 0.05$). Overall, our results suggested that the dual-isotopes
456 method with PWL-corrected $\delta^2\text{H}$ performed best in identifying water uptake patterns.

457 <Table 3>

458 **4. Discussion**

459 *4.1. Possible reasons for isotopic offsets of stem water*

460 Spatial and seasonal disparities of PW-excess values suggested that $\delta^2\text{H}$ offsets of stem
461 water differed greatly during the observation period among the three sites (Fig. 6). A $\delta^2\text{H}$
462 offset could be attributed to methodological issues reported by Orłowski et al. (2018).
463 However, water extraction of soil and stem samples via automatic cryogenic vacuum

464 distillation system was well conducted and yielded a collection rate more than 98% in this
465 study. Contamination of extracted water by organic compounds was also routinely dealt with
466 custom and post-measurement corrections. These techniques extremely avoided the
467 fractionation processes occurring during water extraction. Another possibility for explaining
468 the $\delta^2\text{H}$ offset is the isotopic heterogeneity in plant water pools aroused by discrimination
469 during water transport and redistribution within the plant (Zhao et al., 2016; Barbeta et al.,
470 2020). The $\delta^2\text{H}$ offset would be decreased or even reversed under drier conditions as a result
471 of evaporative enrichment (Barbeta et al., 2020). These studies indicated that there were no
472 $\delta^2\text{H}$ fractionation and offset occurring during root water uptake. However, $\delta^2\text{H}$ offsets were
473 more noticeable under drier conditions in our study (e.g. much lower PW-excess values
474 occurring on May 5 at sites B and C). It was impossible to be completely ascribed to the
475 evaporative enrichment in plant water pools.

476 The $\delta^2\text{H}$ offset of stem water probably occurred in the soil-root interfaces by root water
477 uptake (Allison et al., 1983; Vargas et al., 2017). It was found that large $\delta^2\text{H}$ offset was
478 synchronized to low SWC in the 0–150 cm layer and the decline of water table from May to
479 June (Fig. 4). More interestingly, $\delta^2\text{H}$ offset progressively decreased as SWC in the 0–150 cm
480 layer increased with increasing precipitation amount and rising water table. This might be due
481 to that pore spaces between soil grains and roots increased with the soil water loss under the
482 increase of WTD, which resulted in stronger $\delta^2\text{H}$ fractionation during root water uptake
483 (Barnes and Allison, 1983; Vargas et al., 2017). Moreover, the $\delta^2\text{H}$ offsets at high-SSC sites
484 (mean SSC of 80.7% for site B and 90.8% for site C) were significantly larger than those at
485 low-SSC site (mean SSC of 33.4% for site A) (Table 1 and Fig. 6). It has been reported that
486 $\delta^2\text{H}$ fractionation was controlled by variable diffusive resistance of soil vapors, which was
487 indicated by air filled porosity and the tortuosity of the soil (Barnes and Allison, 1988).
488 Therefore, the high SSC could increase the pore spaces (Barnes and Allison, 1983; Vargas et

489 al., 2017) and possibilities of roots contacting with air during root water uptake, which could
490 lead to $\delta^2\text{H}$ offset (Evaristo et al., 2017; Geris et al., 2017).

491 Previous studies found that soil clay content and/or carbonate content could result in $\delta^{18}\text{O}$
492 fractionation of water added to soil particularly under low soil water content, leading to
493 conflicting results in quantification of root water uptake (Meißner et al., 2014; Yang et al.,
494 2015). The bias of $\delta^{18}\text{O}$ might be caused by oxygen isotope exchanges between soil water
495 and carbonates during the water extraction process. The adsorbed cation isotope effects in
496 mineral–water interface were also examined in greenhouse experiments by Oerter et al.
497 (2014). However, if soil water with depleted $\delta^{18}\text{O}$ values was taken up by roots, stem water
498 should be depleted in both isotopes but not only in $\delta^2\text{H}$ (Barbeta et al., 2019). The stem $\delta^{18}\text{O}$
499 matched those of source water during the growing season of riparian trees and no $\delta^{18}\text{O}$ offset
500 was observed in our study (Fig.5). Lin and Sternberg (1993) and Ellsworth and Williams
501 (2007) reported that passage of water through symplastic pathway led to $\delta^2\text{H}$ fractionation in
502 soil–root interface, but no $\delta^{18}\text{O}$ fractionation was observed during root water uptake, transfer
503 and transport within the plant (Zhao et al., 2016). And a few laboratory experiments
504 confirmed this finding (Vargas et al., 2017; Barbeta et al., 2020). Quite a few studies
505 presented notable isotopic offsets for $\delta^2\text{H}$ rather than for $\delta^{18}\text{O}$ (Zhao et al., 2016; Evaristo et
506 al., 2017; Barbeta et al., 2020). It is mainly due to that the reversible diffusion of water
507 through the ultrafiltration membrane from the external medium to the root xylem
508 discriminates against ^2H about 10 times more than ^{18}O during water uptake (Lin and
509 Sternberg, 1993; Vargas et al., 2017). Nevertheless, the bias of $\delta^{18}\text{O}$ and corresponding
510 reasons need further investigations.

511 *4.2. Correction of $\delta^2\text{H}$ offset for identifications of plant water sources*

512 By means of comparing AIC, BIC and RMSE during the observation period at the three
513 sites, the MixSIAR model outputs with uncorrected $\delta^2\text{H}$ displayed higher AIC, BIC and RMSE

514 values than those with corrected $\delta^2\text{H}$ (Figs. 6 and 7). This indicated that $\delta^2\text{H}$ offsets in stem
515 water greatly affected plant water source contributions estimated using either single or
516 dual-isotopes method. Generally, $\delta^2\text{H}$ offsets lead to underestimation of proportional
517 contributions of deep water sources using uncorrected $\delta^2\text{H}$ (Evaristo et al., 2017; Barbeta et al.,
518 2019). Barbeta et al. (2019) found that dual-isotopes approach with SWL-corrected $\delta^2\text{H}$
519 estimated 1.5 times of the groundwater contribution to stem water than dual-isotopes method
520 with uncorrected $\delta^2\text{H}$. Our study showed that dual-isotopes method with uncorrected $\delta^2\text{H}$
521 underestimated groundwater contribution by 56.3% at shallow WTD sites compared to
522 dual-isotopes method with corrected $\delta^2\text{H}$ (Fig. 7). Moreover, soil water contribution in the
523 0–30 cm layer was underestimated by 30.4% at deep WTD site where groundwater could not
524 be used by plants (Fig. 7). It was evident that the effects of $\delta^2\text{H}$ offsets on quantifying plant
525 water sources were remarkably different among the three sites with various WTDs. Identifying
526 plant water sources should primarily check $\delta^2\text{H}$ offsets especially under the conditions of high
527 SSC and variable WTD fluctuations.

528 The MixSIAR model outputs using single $\delta^{18}\text{O}$ displayed lower AIC, BIC and RMSE
529 values than those using dual-isotopes with uncorrected $\delta^2\text{H}$ (Table 3). This suggested that
530 single $\delta^{18}\text{O}$ performed better than dual-isotopes method with uncorrected $\delta^2\text{H}$ in the attribution
531 of plant water sources when there were notable $\delta^2\text{H}$ offsets of stem water from its potential
532 sources (Goebel et al., 2015; Evaristo et al., 2017; Vargas et al., 2017; Barbeta et al., 2019).
533 However, the MixSIAR model outputs estimated using single $\delta^{18}\text{O}$ were greatly different with
534 those estimated using dual-isotopes with PWL-corrected $\delta^2\text{H}$ method on several sampling
535 campaigns especially at sites B and C (Fig. 7 and Table S1). The differences would be enlarged
536 with the increase of $\delta^2\text{H}$ offsets as indicated by Barbeta et al.(2019). It was evident that the
537 single $\delta^{18}\text{O}$ method showed larger uncertainties (RMSE of 7.0%) for plant source water
538 identifications over the observation period than the dual-isotopes with PWL-corrected $\delta^2\text{H}$

539 method (RMSE of 4.8%). Moreover, the single $\delta^{18}\text{O}$ method could lead to erroneous
540 interpretations when root water uptake took place simultaneously from several zones, while
541 dual-isotopes method might provide information that was not apparent in the single isotope
542 method (Evaristo et al., 2017).

543 Furthermore, the source contributions estimated using dual-isotopes with PWL-corrected
544 $\delta^2\text{H}$ method had closer correlations with the environmental variables indicating by lower AIC
545 and BIC values (Table 3). That is, when the isotopic offsets were corrected and the isotopes in
546 stem water did not deviated from their corresponding water sources, the MixSIAR model with
547 dual isotopes was more accurate to identify water sources than that with single $\delta^{18}\text{O}$ isotope.
548 Parnell et al. (2010) also reported that increasing the number of isotopes without $\delta^2\text{H}$ offsets
549 could improve the predictive accuracy of the Bayesian model, when the number of sources
550 (e.g., five water sources for trees in this study) were more than that of tracer isotopes.
551 Therefore, it is essential to propose a correction method to correct the $\delta^2\text{H}$ offsets rather than
552 just use $\delta^{18}\text{O}$ for plant water source identifications.

553 The MixSIAR model outputs estimated using dual-isotopes with PWL-corrected $\delta^2\text{H}$
554 method displayed lower AIC, BIC, and RMSE values than those using dual-isotopes with
555 SWL-corrected $\delta^2\text{H}$ method (Table 3). It suggested that dual-isotopes method with
556 PWL-corrected $\delta^2\text{H}$ performed better in plant water source estimations than that with
557 SWL-corrected $\delta^2\text{H}$. The reason was probably due to that groundwater was a crucial and
558 independent water source for *S. babylonica* growing in areas with shallow WTD. Low
559 precipitation and shallow groundwater with abundant dissolved oxygen and nutrients during
560 the growing season of *S. babylonica* could stimulate deep roots to tap into capillary fringe or
561 even water tables to take up groundwater directly to meet the water requirement (Yu et al.,
562 2017). Therefore, both groundwater and soil water should be in consideration of correcting
563 stem water $\delta^2\text{H}$ offsets especially for phreatophytes in shallow WTD areas. The PWL

564 correction method was more accurate and avoided an underestimation of groundwater
565 contribution (mean of 5.0 %) in comparison to the SWL correction method.

566 In summary of previous and our results, we propose four distinct types of $\delta^2\text{H}$ offsets and
567 the corresponding correction methods based on different WTDs and groundwater recharge
568 sources for riparian trees (Fig. 8). There is one thing in common among these four types: the
569 contributions of plant water sources estimated using $\delta^2\text{H}$ are not in agreement with those
570 estimated using $\delta^{18}\text{O}$ due to stem water $\delta^2\text{H}$ offsets (Barbeta et al., 2020). On the one hand,
571 when groundwater recharge mainly comes from precipitation, the isotopic composition of
572 groundwater is generally more depleted than that of soil water at different layers (Figs. 8a and
573 8b). $\delta^2\text{H}$ offset characteristics depends on whether $\delta^{18}\text{O}$ in stem water is within the range of that
574 in groundwater or not. For instance, when groundwater cannot be taken up by plants under
575 deep WTD conditions, $\delta^{18}\text{O}$ in stem water is not within the range of that in groundwater as
576 observed in previous studies (Brooks et al., 2010; Evaristo et al., 2017) and at site A in this
577 study (Fig. 8a). Consequently, groundwater will not be considered to correct $\delta^2\text{H}$ offset. In case
578 that groundwater serves as an important water source for riparian trees in shallow WTD areas
579 (Oerter and Bowen, 2019), both groundwater and soil water should be taken into consideration
580 to correct $\delta^2\text{H}$ offset (i.e., PWL correction method) (Fig. 8b). On the other hand, groundwater is
581 principally recharged by seepage of surface water, which may lead to more enriched isotopic
582 composition of groundwater compared to the depleted soil water in deep layers (Figs. 8c and
583 8d). If $\delta^{18}\text{O}$ in stem water is within the range of that in groundwater such as at sites B and C in
584 our study and in other field studies (Bowling et al., 2017; Barbeta et al., 2019), groundwater
585 should be considered to correct $\delta^2\text{H}$ offset (Fig. 8d). Otherwise, when $\delta^{18}\text{O}$ in stem water is not
586 within the range of that in groundwater (Fig. 8c), groundwater is not included in one of the
587 water sources to correct $\delta^2\text{H}$ offset. Therefore, the proposed PWL correction method in this

588 study considers all potential water sources, and can be applied to quantify root water uptake
589 under different types of $\delta^2\text{H}$ offsets of stem water.

590 <Figure 8>

591 4.3. Implications

592 Riparian trees perennially or seasonally depended on groundwater in the arid and semi-arid
593 climate regions (Fan, 2015; Contreras et al., 2011; Miguez-Macho and Fan, 2012) or
594 Mediterranean climate region (Dawson and Pate, 1996). There could be an underestimation of
595 groundwater contributions when using uncorrected $\delta^2\text{H}$ due to $\delta^2\text{H}$ offset, which could be
596 resolved by the developed PWL correction method in this study. When groundwater served as
597 a crucial water source, the PWL correction method performed better than both the SWL
598 correction method and non-correction method in identifications of plant water sources. It was
599 evident that MixSIAR model using dual isotopes with PWL-corrected $\delta^2\text{H}$ estimated more
600 accurate proportional contributions of groundwater.

601 In this study, only possible reasons for $\delta^2\text{H}$ offsets of stem water from its potential sources
602 was deducted by indirect evidences. The mechanisms of $\delta^2\text{H}$ offsets requires further
603 investigation by collecting different plant water pools from roots, xylem sap as well as stem
604 tissues under various soil texture and water table conditions. The potential water sources might
605 not be confined to soil water and groundwater in some regions. They also included other
606 sources such as rock moisture, fog water, and dew water (Wang et al., 2017a; Wang et al.,
607 2019b). Only when all potential water sources were considered to fit the correction line, the
608 MixSIAR model with PWL-corrected input data could obtain more accurate estimations of
609 plant water sources contributions. The PWL correction method was evaluated for determining
610 riparian tree water sources only considering soil water and groundwater sources in this study.
611 It requires further validation using more cases in consideration of other water sources
612 including rock moisture, fog water and dew water. The PWL correction method provides

613 insights into determining accurate root water uptake patterns even if $\delta^2\text{H}$ offset exists. It further
614 contributes to understanding the relationship between plants and water such as partitioning
615 evapotranspiration fluxes into transpiration and evaporation (Wang et al., 2010), water
616 competition among different plant species (Wang et al., 2017b), species' abilities to respond to
617 variable hydrological conditions (Wu et al., 2019b), or even the parameterization of
618 ecohydrological models at both plot and catchment scales (Miller et al., 2012; Beyer et al.,
619 2016; Sprenger et al., 2018).

620 **5. Conclusions**

621 In this study, the PWL correction method was proposed to correct the $\delta^2\text{H}$ offsets of stem
622 water from its potential water sources. The MixSIAR model coupled with dual stable isotopes
623 ($\delta^2\text{H}$ and $\delta^{18}\text{O}$) were used to determine seasonal variations in water uptake patterns of riparian
624 trees (*S. babylonica*) at three sites in 2019 along the Jian and Chaobai River in Beijing, China.
625 When using dual-isotopes method with $\delta^2\text{H}$ in stem water corrected by the PWL, the average
626 contributions of soil water in the 0–30, 30–80, 80–150, 150–300 cm layers and groundwater
627 were 22.4%, 18.3%, 14.1%, 16.7% and 28.5%, respectively. Riparian trees mainly used soil
628 water below 150 cm depth on May 5, June 14, July 26, and August 15 with contributions
629 greater than 54.6%, then the main root water uptake depth returned to the 0–150 cm layer on
630 September 26 and November 5 with contributions more than 60.5%. Different types of input
631 data led to considerable differences in the contributions of soil water in the 0–30 cm layer
632 (9.9–57.6%) and water sources below the depth of 80 cm (29.0–76.4%) especially when $\delta^2\text{H}$
633 offset was pronounced. The MixSIAR model with dual-isotopes method was more accurate to
634 identify plant water sources than that with single-isotope method. The best performance of
635 PWL correction method was underlined compared to SWL correction and non-correction
636 methods when groundwater was accessible for plants. Furthermore, four distinct types of $\delta^2\text{H}$
637 offsets in riparian zone and their correspondingly suitable correction methods have been

638 summarized. This study provides crucial insights into exploring accurate root water uptake
639 patterns to account for $\delta^2\text{H}$ offset of stem water.

640

641 **Acknowledgements**

642 This work was supported by the National Natural Science Foundation of China (41730749,
643 41671027). LW acknowledges partial support from the Division of Earth Sciences of National
644 Science Foundation (EAR-1554894). Sincere thanks go to Xue Zhang, Lihu Yang, Binghua
645 Li and Zekang He for their assistance in experiments. We are grateful to the associate editor
646 and anonymous reviewers for their comments to improve this manuscript.

647

648 **References**

- 649 Allison, G.B., Barnes, C.J., Hughes, M.W., 1983. The distribution of deuterium and ^{18}O in
650 dry soils 2. experimental. *Journal of Hydrology*. 64, 377-397.
- 651 Asbjornsen, H., Mora, G., Helmers, M.J., 2007. Variation in water uptake dynamics among
652 contrasting agricultural and native plant communities in the Midwestern U.S. *Agriculture,*
653 *Ecosystems and Environment*. 121, 343-356.
- 654 Barbeta, A., Gimeno, T.E., Clave, L., Frejaville, B., Jones, S.P., Delvigne, C., Wingate, L.,
655 Ogee, J., 2020. An explanation for the isotopic offset between soil and stem water in a
656 temperate tree species. *New Phytologist*. 227, 766-779.
- 657 Barbeta, A., Jones, S.P., Clavé, L., Wingate, L., Gimeno, T.E., Fréjaville, B., Wohl, S., Ogee,
658 J., 2019. Unexplained hydrogen isotope offsets complicate the identification and
659 quantification of tree water sources in a riparian forest. *Hydrology and Earth System*
660 *Sciences*. 23, 2129-2146.
- 661 Barnes, C.J., Allison, G.B., 1983. The distribution of deuterium and ^{18}O in dry soils.1. Theory.
662 *Journal of Hydrology*. 60, 141-156.

663 Barnes, C.J., Allison, G.B., 1988. Tracing of water-movement in the unsaturated zone using
664 stable isotopes of hydrogen and oxygen. *Journal of Hydrology*. 100, 143-176.

665 Beyer, M., Koeniger, P., Gaj, M., Hamutoko, J.T., Wanke, H., Himmelsbach, T., 2016. A
666 deuterium-based labeling technique for the investigation of rooting depths, water uptake
667 dynamics and unsaturated zone water transport in semiarid environments. *Journal of*
668 *Hydrology*. 533, 627-643.

669 Bowling, D.R., Schulze, E.S., Hall, S.J., 2017. Revisiting streamside trees that do not use
670 stream water: Can the two water worlds hypothesis and snowpack isotopic effects explain
671 a missing water source? *Ecohydrology*. 10, 1-12.

672 Brooks, J.R., Barnard, H.R., Coulombe, R., McDonnell, J.J., 2010. Ecohydrologic separation
673 of water between trees and streams in a Mediterranean climate. *Nature Geoscience*. 3,
674 100-104.

675 Christina, M., le Maire, G., Nouvellon, Y., Vezy, R., Bordon, B., Battie-Laclau, P., Goncalves,
676 J.L.M., Delgado-Rojas, J.S., Bouillet, J.P., Laclau, J.P., 2018. Simulating the effects of
677 different potassium and water supply regimes on soil water content and water table depth
678 over a rotation of a tropical *Eucalyptus grandis* plantation. *Forest Ecology and*
679 *Management*. 418, 4-14.

680 Contreras, S., Jobbágy, E.G., Villagra, P.E., Noretto, M.D., Puigdefábregas, J., 2011. Remote
681 sensing estimates of supplementary water consumption by arid ecosystems of central
682 Argentina. *Journal of Hydrology*. 397, 10-22.

683 Dawson, T.E., Ehleringer, J.R., 1991. Streamside trees that do not use stream water. *Nature*.
684 350, 335-337.

685 Dawson, T.E., Ehleringer, J.R., 1993. Isotopic enrichment of water in the 'woody' tissues:
686 Implications for plant water source, water uptake, and other studies which use the stable
687 isotopic composition of cellulose. *Geochimica et Cosmochimica. Acta*. 57, 3487-3492.

688 Dawson, T.E., Pate, J.S., 1996. Seasonal water uptake and movement in root systems of
689 Australian phraeatophytic plants of dimorphic root morphology: a stable isotope
690 investigation. *Oecologia*. 107, 13-20.

691 Ehleringer, J.R., Dawson, T.E., 1992. Water uptake by plants: perspectives from stable
692 isotope composition. *Plant, Cell and Environment*. 15, 1073-1082.

693 Ellsworth, P.Z., Williams, D.G., 2007. Hydrogen isotope fractionation during water uptake by
694 woody xerophytes. *Plant and Soil*. 291, 93-107.

695 Evaristo, J., Jasechko, S., McDonnell, J.J., 2015. Global separation of plant transpiration
696 from groundwater and streamflow. *Nature*. 525, 91-107.

697 Evaristo, J., McDonnell, J.J., Clemens, J., 2017. Plant source water apportionment using
698 stable isotopes: A comparison of simple linear, two-compartment mixing model
699 approaches. *Hydrological Processes*. 31, 3750-3758.

700 Fan, Y., 2015. Groundwater in the Earth's critical zone: Relevance to large-scale patterns and
701 processes. *Water Resources Research*. 51, 3052-3069.

702 Ferro, A., Gefell, M., Kjelgren, R., Lipson, D.S., Zollinger, N., Jackson, S., 2003.
703 Maintaining hydraulic control using deep rooted tree systems. In: Tsao, D. (Eds).
704 *Advances in Biochemical Engineering-Biotechnology*. Springer-Verlag., Berlin, pp.
705 125-156.

706 Geris, J., Tetzlaff, D., McDonnell, J.J., Soulsby, C., 2017. Spatial and temporal patterns of
707 soil water storage and vegetation water use in humid northern catchments. *Science of the*
708 *Total Environment*. 595, 486-493.

709 Goebel, T.S., Lascano, R.J., Paxton, P.R., Mahan, J.R., 2015. Rainwater use by irrigated
710 cotton measured with stable isotopes of water. *Agricultural Water Management*. 158,
711 17-25.

712 Good, S.P., Noone, D., Bowen, G., 2015. Hydrologic connectivity constrains partitioning of

713 global terrestrial water fluxes. *Science*. 349, 175-177.

714 Gou, S., Miller, G., 2014. A groundwater-soil-plant-atmosphere continuum approach for
715 modelling water stress, uptake, and hydraulic redistribution in phreatophytic vegetation.
716 *Ecohydrology*. 7, 1029-1041.

717 Jiao, L., Lu, N., Fang, W.W., Li, Z.S., Wang, J., Jin, Z., 2019. Determining the independent
718 impact of soil water on forest transpiration: A case study of a black locust plantation in
719 the Loess Plateau, China. *Journal of Hydrology*. 572, 671-681.

720 Landwehr, J.M., Coplen, T.B., 2006. Line-conditioned excess: a new method for
721 characterizing stable hydrogen and oxygen isotope ratios in hydrologic systems. *Isotopes*
722 *in Environmental Studies*. 92, 132-135.

723 Lin, G.H., Sternberg, L.D.L., 1993. Hydrogen Isotopic Fractionation by Plant Roots during
724 Water Uptake in Coastal Wetland Plants. In: Ehleringer, J.R., Hall, A.E. and Farquhar,
725 G.D. (Eds). *Stable Isotopes and Plant Carbon-Water Relation*. Academic Press Inc, New
726 York, pp. 497-510.

727 Ma, Y., Song, X.F., 2016. Using stable isotopes to determine seasonal variations in water
728 uptake of summer maize under different fertilization treatments. *Science of the Total*
729 *Environment*. 550, 471-483.

730 Markus-Michalczyk, H., Zhu, Z.C., Bouma, T.J., 2019. Morphological and biomechanical
731 responses of floodplain willows to tidal flooding and salinity. *Freshwater Biology*. 64,
732 913-925.

733 Martorello, A.S.Q., Fernandez, M.E., Monterubbianesi, M.G., Colabelli, M.N., Laclau, P.,
734 Gyenge, J.E., 2020. Effect of combined stress (salinity + hypoxia) and auxin rooting
735 hormone addition on morphology and growth traits in six *Salix* spp. clones. *New Forests*.
736 51, 61-80.

737 Meißner, M., Köhler, M., Schwendenmann, L., Hölscher, D., Dyckmans, J., 2014. Soil water

738 uptake by trees using water stable isotopes ($\delta^2\text{H}$ and $\delta^{18}\text{O}$)—a method test regarding soil
739 moisture, texture and carbonate. *Plant and Soil*. 376, 327-335.

740 Miguez-Macho, G., Fan, Y., 2012. The role of groundwater in the Amazon water cycle: 1.
741 Influence on seasonal streamflow, flooding and wetlands. *Journal of Geophysical*
742 *Research: Atmospheres*. 117, 1-30.

743 Miller, G.R., Cable, J.M., McDonald, A.K., Bond, B., Franz, T.E., Wang, L.X., Gou, S., Tyler,
744 A.P., Zou, C.B., Scott, R.L., 2012. Understanding ecohydrological connectivity in
745 savannas: a system dynamics modelling approach. *Ecohydrology*. 5, 200-220.

746 Oerter, E.J., Bowen, G.J., 2019. Spatio-temporal heterogeneity in soil water stable isotopic
747 composition and its ecohydrologic implications in semiarid ecosystems. *Hydrological*
748 *Processes*. 33, 1724-1738.

749 Oerter, E., Finstad, K., Schaefer, J., Goldsmith, G.R., Dawson, T., Amundson, R., 2014.
750 Oxygen isotope fractionation effects in soil water via interaction with cations (Mg, Ca, K,
751 Na) adsorbed to phyllosilicate clay minerals. *Journal of Hydrology*. 515, 1-9.

752 Orłowski, N., Breuer, L., Angeli, N., Boeckx, P., McDonnell, J.J., 2018. Inter-laboratory
753 comparison of cryogenic water extraction systems for stable isotope analysis of soil water.
754 *Hydrology & Earth System Sciences*. 22, 3619-3637.

755 Parnell, A.C., Inger, R., Bearhop, S., Jackson, A.L., 2010. Source partitioning using stable
756 isotopes: Coping with too much variation. *PLoS ONE*. 5, 1-5.

757 Qian, J., Zheng, H., Wang, P.F., Liao, X.L., Wang, C., Hou, J., Ao, Y.H., Shen, M.M., Liu, J.J.,
758 Li, K., 2017. Assessing the ecohydrological separation hypothesis and seasonal variations
759 in water use by *Ginkgo biloba* L. in a subtropical riparian area. *Journal of Hydrology*. 553,
760 486-500.

761 Rascher, U., Bobich, E.G., Lin, G.H., Walter, A., Morris, T., Naumann, M., Nichol, C.J.,
762 Pierce, D., Bil, K., Kudryarov, V., Berry, J.A., 2004. Functional diversity of

763 photosynthesis during drought in a model tropical rainforest - the contributions of leaf
764 area, photosynthetic electron transport and stomatal conductance to reduction in net
765 ecosystem carbon exchange. *Plant Cell and Environment*. 27, 1239-1256.

766 Rothfuss, Y., Javaux, M., 2017. Reviews and syntheses: Isotopic approaches to quantify root
767 water uptake: a review and comparison of methods. *Biogeosciences*. 14, 2199-2224.

768 Song, L.N., Zhu, J.J., Li, M.C., Zhang, J.X., Lv, L.Y., 2016. Sources of water used by *Pinus*
769 *sylvestris* var. *mongolica* trees based on stable isotope measurements in a semiarid sandy
770 region of Northeast China. *Agricultural Water Management*. 164, 281-290.

771 Song, X.F., Tang, Y., Zhang, Y.H., Ma, Y., Han, D., Bu, H., Liu, F., 2017. Using stable
772 isotopes to study vapor transport of continuous precipitation in Beijing. *Advances in*
773 *Water Science*. 28, 488-495 (in Chinese).

774 Sprenger, M., Tetzlaff, D., Buttle, J., Laudon, H., Leister, H., Mitchell, C.P.J., Snelgrove, J.,
775 Weiler, M., Soulsby, C., 2018. Measuring and modeling stable isotopes of mobile and bulk
776 soil water. *Vadose Zone Journal*. 17, 1-18.

777 Stock, B.C., Semmens, B.X., 2013. MixSIAR GUI User Manual, version 1.0.
778 <http://conserver.iugo-cafe.org/user/brice.semmens/MixSIAR>.

779 Vargas, A.I., Schaffer, B., Li, Y.H., Sternberg, L.S.L., 2017. Testing plant use of mobile vs
780 immobile soil water sources using stable isotope experiments. *New Phytologist*. 215,
781 582-594.

782 Vereecken, H., Huisman, J.A., Franssen, H.J.H., Bruggemann, N., Bogaen, H.R., Kollet, S.,
783 Javaux, M., van der Kruk, J., Vanderborght, J., 2015. Soil hydrology: Recent
784 methodological advances, challenges, and perspectives. *Water Resources Research*. 51,
785 2616-2633.

786 Vincke, C., Thiry, Y., 2008. Water table is a relevant source for water uptake by a Scots pine
787 (*Pinus sylvestris* L.) stand: Evidences from continuous evapotranspiration and water table

788 monitoring. *Agricultural and Forest Meteorology*. 148, 1419-1432.

789 Wang, J., Fu, B.J., Lu, N., Li, Z., 2017b. Seasonal variation in water uptake patterns of three
790 plant species based on stable isotopes in the semi-arid Loess Plateau. *Science of the Total*
791 *Environment*. 609, 27-37.

792 Wang, J., Lu, N., Fu, B.J., 2019a. Inter-comparison of stable isotope mixing models for
793 determining plant water source partitioning. *Science of the Total Environment*. 666,
794 685-693.

795 Wang, L.X., Caylor, K.K., Dragoni, D., 2009. On the calibration of continuous,
796 high-precision $\delta^{18}\text{O}$ and $\delta^2\text{H}$ measurements using an off-axis integrated cavity output
797 spectrometer. *Rapid Communications in Mass Spectrometry*. 23, 530-536.

798 Wang, L.X., Caylor, K.K., Villegas, J.C., Barron-Gafford, G.A., Breshears, D.D., Huxman,
799 T.E., 2010. Partitioning evapotranspiration across gradients of woody plant cover:
800 Assessment of a stable isotope technique. *Geophysical Research Letters*. 37, L09401,
801 doi:10.1029/2010GL043228.

802 Wang, L.X., Good, S.P., Caylor, K.K., 2014. Global synthesis of vegetation control on
803 evapotranspiration partitioning. *Geophysical Research Letters*. 41, 6753-6757.

804 Wang, L.X., Kaseke, K.F., Ravi, S., Jiao, W.Z., Mushi, R., Shuuya, T., Maggs-Kolling, G.,
805 2019b. Convergent vegetation fog and dew water use in the Namib Desert. *Ecohydrology*.
806 12, e2130, doi:10.1002/eco.2130.

807 Wang, L.X., Kaseke, K.F., Seely, M.K., 2017a. Effects of non-rainfall water inputs on
808 ecosystem functions. *Wiley Interdisciplinary Reviews-Water*. 4, e1179,
809 doi:10.1002/wat2.1179.

810 Wei, Z.W., Yoshimura, K., Wang, L.X., Miralles, D.G., Jasechko, S., Lee, X.H., 2017.
811 Revisiting the contribution of transpiration to global terrestrial evapotranspiration.
812 *Geophysical Research Letters*. 44, 2792-2801.

813 Wu, H.W., Zhao, G.Q., Li, X.Y., Wang, Y., He, B., Jiang, Z.Y., Zhang, S.Y., Sun, W., 2019b.
814 Identifying water sources used by alpine riparian plants in a restoration zone on the
815 Qinghai-Tibet Plateau: Evidence from stable isotopes. *Science of the Total Environment*.
816 697, 134092, doi: 10.1016/j.scitotenv.2019.134092.

817 Wu, X., Zheng, X.J., Yin, X.W., Yue, Y.M., Liu, R., Xu, G.Q., Li, Y., 2019a. Seasonal
818 variation in the groundwater dependency of two dominant woody species in a desert
819 region of Central Asia. *Plant and Soil*. 444, 39-55.

820 Yang, B., Wen, X.F., Sun, X.M., 2015a. Irrigation depth far exceeds water uptake depth in an
821 oasis cropland in the middle reaches of Heihe River Basin. *Sci. Rep.* 5, 15206.
822 <http://dx.doi.org/10.1038/srep15206>.

823 Yang, B., Wen, X.F., Sun, X.M., 2015b. Seasonal variations in depth of water uptake for a
824 subtropical coniferous plantation subjected to drought in an East Asian monsoon region.
825 *Agricultural and Forest Meteorology*. 201, 218-228.

826 Yang, B., Wang, P.Y., You, D.B., Liu, W.J., 2018. Coupling evapotranspiration partitioning
827 with root water uptake to indentify the water consumption characteristics of winter wheat:
828 A case study in the North China Plain. *Agricultural and Forest Meteorology*. 259,
829 296-304.

830 Yu, Y.L., Song, X.F., Zhang, Y.H., Zheng, F.D., Liu, L.C., 2017. Impact of reclaimed water in
831 the watercourse of Huai River on groundwater from Chaobai River basin, Northern China.
832 *Frontiers of Earth Science*. 11, 643-659.

833 Zhao, L.J., Wang, L.X., Cernusak, L.A., Liu, X.H., Xiao, H.L., Zhou, M.X., Zhang, S.Q.,
834 2016. Significant difference in hydrogen isotope composition between xylem and tissue
835 water in *Populus Euphratica*. *Plant, Cell and Environment*. 39, 1848-1857.

836 Zhao, L.J., Xiao H.L., Zhou, J., Wang, L.X., Cheng, G.D., Zhou, M.X., Yin, L., McCabe,
837 M.F., 2011. Detailed assessment of isotope ratio infrared spectroscopy and isotope ratio

838 mass spectrometry for the stable isotope analysis of plant and soil waters. Rapid
839 Communications in Mass Spectrometry. 25, 3071-3082.

840 Zipper, S.C., Soylu, M.E., Booth, E.G., Loheide, S.P., 2015. Untangling the effects of shallow
841 groundwater and soil texture as drivers of subfield-scale yield variability. Water
842 Resources Research. 51, 6338-6358.

843

844 **Figure captions**

845 Fig. 1. The illustration for $\delta^2\text{H}$ offsets of the stem water from its potential water sources that
846 derived from soil water line (SWL) and potential water source line (PWL). The $\delta^2\text{H}$
847 offsets of the stem water enclosed by a yellow square are corrected by SW-excess
848 ($Y1-Y2$) and PW-excess ($Y1-Y3$), respectively.

849 Fig. 2. Schematic diagram for the the study area and the three sampling sites (A, B, and C) , and
850 the pictures of experimental plots at site C.

851 Fig. 3. Changes of (a) daily precipitation and daily vapor pressure deficit (VPD) in the study
852 area, (b) water table depth (WTD) at sites A, B, and C during the observation period
853 in 2019.

854 Fig. 4. The SWC in different soil layers at sites (a) A, (b) B, and (c) C during the observation
855 period in 2019. The box lines represent mean and standard deviation values (SD),
856 whiskers indicate maximum and minimum values, and black diamonds are outliers.

857 Fig. 5. Dual-isotopes ($\delta^2\text{H}$ and $\delta^{18}\text{O}$) plots of stem water of the riparian trees and their
858 potential water sources (soil water in different layers, precipitation, groundwater, and
859 river water) at sites (a) A, (b) B, and (c) C on six sampling campaigns during the
860 observation period. The significant levels of all SWL and PWL are less than 0.001 (p
861 < 0.001).

862 Fig. 6. Seasonal variations in (a) the PW-excess and (b) SW-excess of riparian trees at sites A,
863 B, and C in 2019. The PW-excess value is as the same as the SW-excess value at site
864 A. The box lines represent means and standard deviations (SD), whiskers indicate
865 maximum and minimum values, and black diamonds are outliers.

866 Fig. 7. Seasonal water uptake patterns for riparian trees at three representative sites A, B, and
867 C estimated via the MixSIAR model incorporating with (a) uncorrected $\delta^2\text{H}$ and $\delta^{18}\text{O}$,
868 (b) uncorrected $\delta^2\text{H}$, (c) $\delta^{18}\text{O}$, (d) $\delta^2\text{H}$ corrected by SWL and $\delta^{18}\text{O}$, (e) $\delta^2\text{H}$ corrected

869 by SWL, (f) $\delta^2\text{H}$ corrected by PWL and $\delta^{18}\text{O}$, and (g) $\delta^2\text{H}$ corrected by PWL. The
870 MixSIAR model outputs using PWL correction method is same with those using SWL
871 correction method at site A.

872 Fig. 8. Different types of $\delta^2\text{H}$ offset between stem water and its potential water sources shown
873 in dual-isotopes ($\delta^2\text{H}$ and $\delta^{18}\text{O}$) plots. The potential water sources in the shaded area
874 represent main water sources of the enclosed stem water sample by the red square. The
875 red star represents the $\delta^2\text{H}$ -corrected stem water which derives from the enclosed stem
876 water by the red square.

Table 1. Soil particle size and soil texture at different depths at the three sites.

Site	Depth (cm)	Soil particle size (%)			Soil texture
		Clay	Silt	Sand	
Site A	0–30	5.8	46.8	47.4	Clay loam
	30–80	8.5	70.3	21.2	Clay loam
	80–150	7.5	62.0	30.5	Clay loam
	150–300	6.8	56.5	34.5	Clay loam
Site B	0–30	1.3	17.3	81.4	Sandy loam
	30–80	1.2	17.8	81.0	Sandy loam
	80–150	1.6	21.1	77.4	Sandy loam
	150–300	0.9	16.2	82.9	Sandy loam
Site C	0–30	0.6	14.9	84.5	Sand
	30–80	0.1	7.9	92.0	Sand
	80–150	0.1	6.9	93.0	Sand
	150–300	0.1	6.1	93.8	Sand

Table 2. Proportions of potential water source contributions to riparian trees estimated by MixSIAR model incorporating with seven types of isotope data.

Input data modes	Proportional contributions (%)									
	0-30 cm		30-80 cm		80-150 cm		150-300 cm		Groundwater	
	Mean	SD	Mean	SD	Mean	SD	Mean	SD	Mean	SD
$\delta^2\text{H} + \delta^{18}\text{O}$	27.6	13.2	30.3	9.2	16.7	2.8	12.6	2.8	12.9	4.6
$\delta^2\text{H}$	16.7	8.9	31.1	13.6	22.4	7.1	17.0	5.5	12.9	4.1
$\delta^{18}\text{O}$	22.3	4.9	20.2	7.2	13.7	5.5	16.4	4.5	27.4	7.7
$\delta^2\text{H}$ (corrected by SWL) + $\delta^{18}\text{O}$	21.4	6.8	19.7	4.4	16.5	7.5	17.9	5.5	24.5	7.5
$\delta^2\text{H}$ (corrected by SWL)	17.4	7.5	18.8	1.8	18.9	6.2	21.1	4.8	23.7	3.1
$\delta^2\text{H}$ (corrected by PWL) + $\delta^{18}\text{O}$	22.4	5.0	18.3	6.1	14.1	6.5	15.7	5.1	29.5	7.4
$\delta^2\text{H}$ (corrected by PWL)	19.3	9.0	15.5	4.2	14.9	4.4	19.7	6.0	30.6	6.6

Table 3. Performances of the seven types of isotope data to estimate water source contributions of riparian trees by the MixSIAR model.

Input data modes	AIC	BIC	RMSE (%)
$\delta^2\text{H} + \delta^{18}\text{O}$	101.7	99.5	9.5
$\delta^2\text{H}$	101.7	99.5	12.4
$\delta^{18}\text{O}$	94.9	92.6	7.0
$\delta^2\text{H}$ (corrected by SWL) + $\delta^{18}\text{O}$	97.6	95.4	5.3
$\delta^2\text{H}$ (corrected by SWL)	96.2	94.0	5.5
$\delta^2\text{H}$ (corrected by PWL) + $\delta^{18}\text{O}$	94.1	91.9	4.8
$\delta^2\text{H}$ (corrected by PWL)	98.0	95.8	8.1

Note: The Akaike Information Criterion (AIC) and Bayesian Information Criterion (BIC) values represent the correlation between water source contributions to stem water and environment variables. The Root Mean Square Error (RMSE) values represent the deviations of the source contributions estimated by one certain input data from the average values of all types of input data.

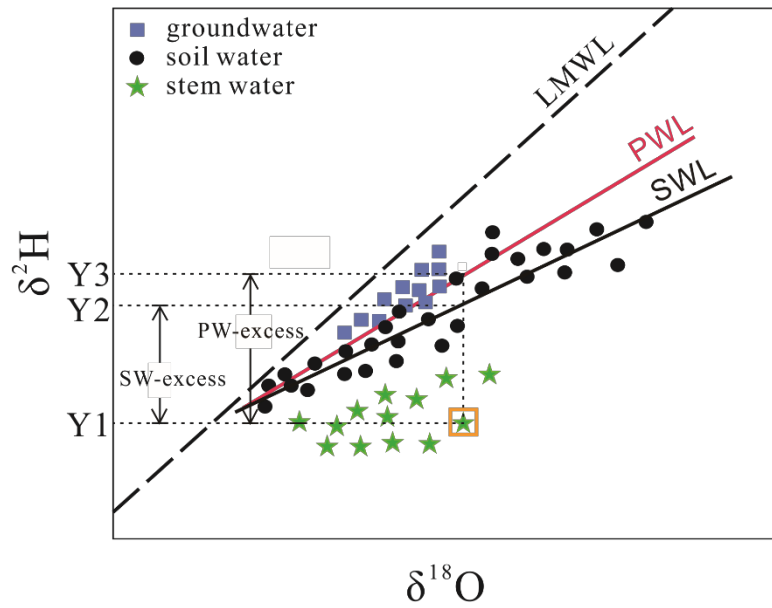


Fig. 1. The illustration for $\delta^2\text{H}$ offsets of the stem water from its potential water sources that derived from soil water line (SWL) and potential water source line (PWL). The $\delta^2\text{H}$ offsets of the stem water enclosed by a yellow square are corrected by SW-excess ($Y1-Y2$) and PW-excess ($Y1-Y3$), respectively.

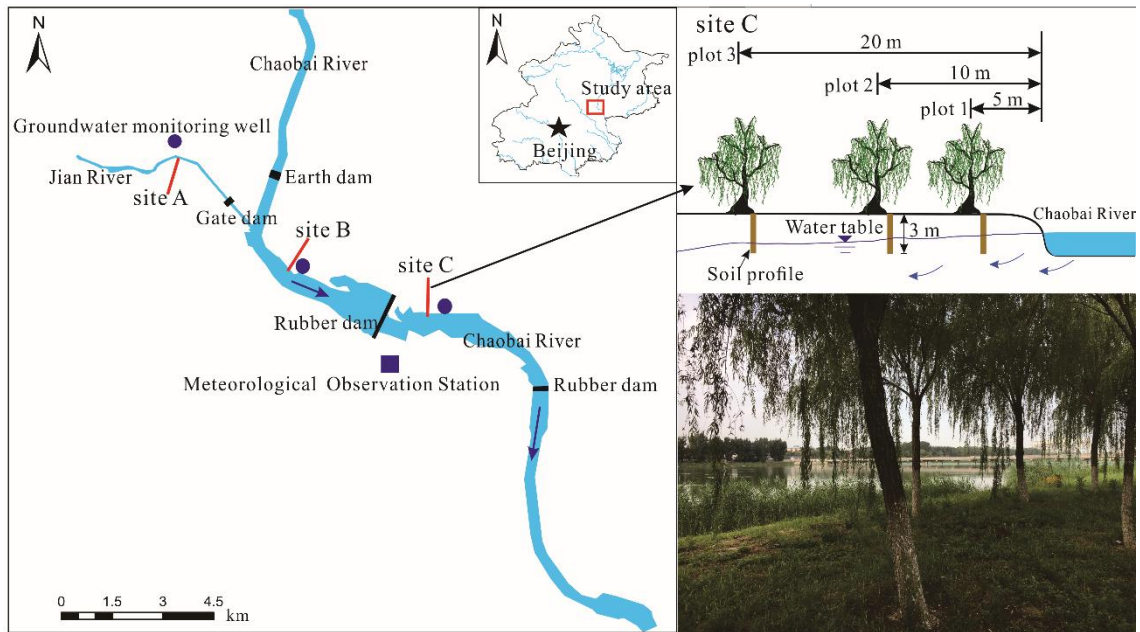


Fig. 2. Schematic diagram for the the study area and the three sampling sites (A, B, and C) , and the pictures of experimental plots at site C.

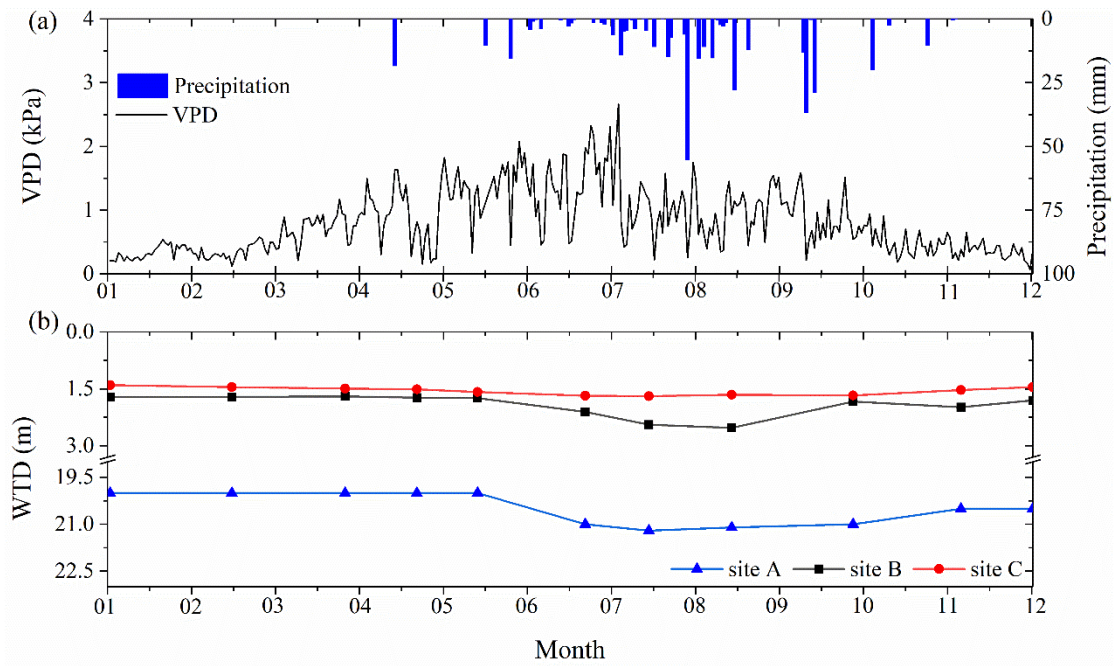


Fig. 3. Changes of (a) daily precipitation and daily vapor pressure deficit (VPD) in the study area, (b) water table depth (WTD) at sites A, B, and C during the observation period in 2019.

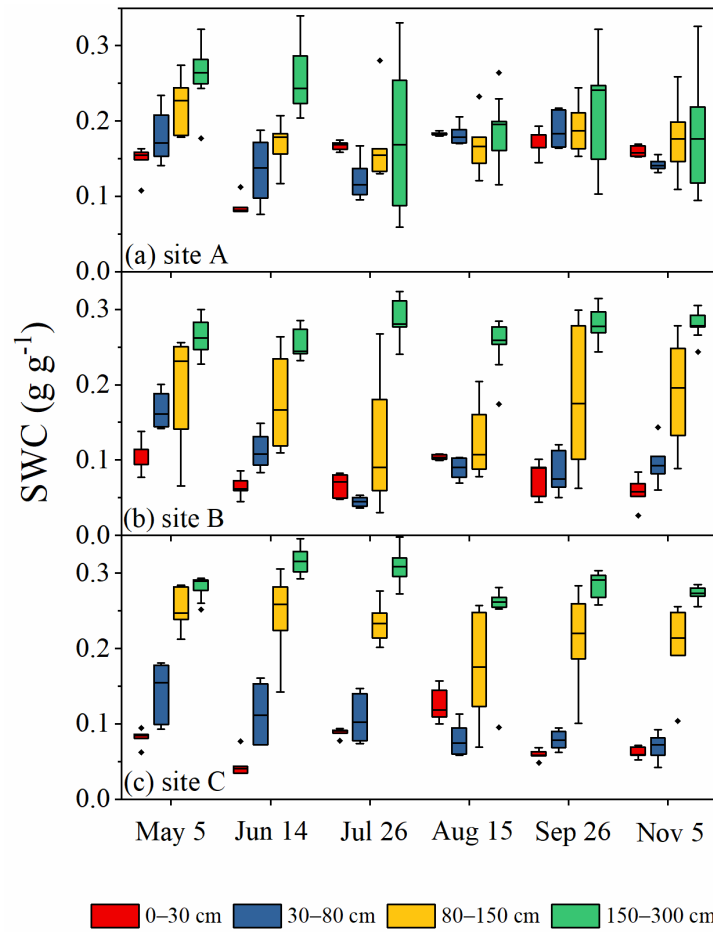


Fig. 4. The soil water content (SWC) in different soil layers at sites (a) A, (b) B, and (c) C during the observation period in 2019. The box lines represent means and standard deviations (SD), whiskers indicate maximum and minimum values, and black diamonds are outliers.

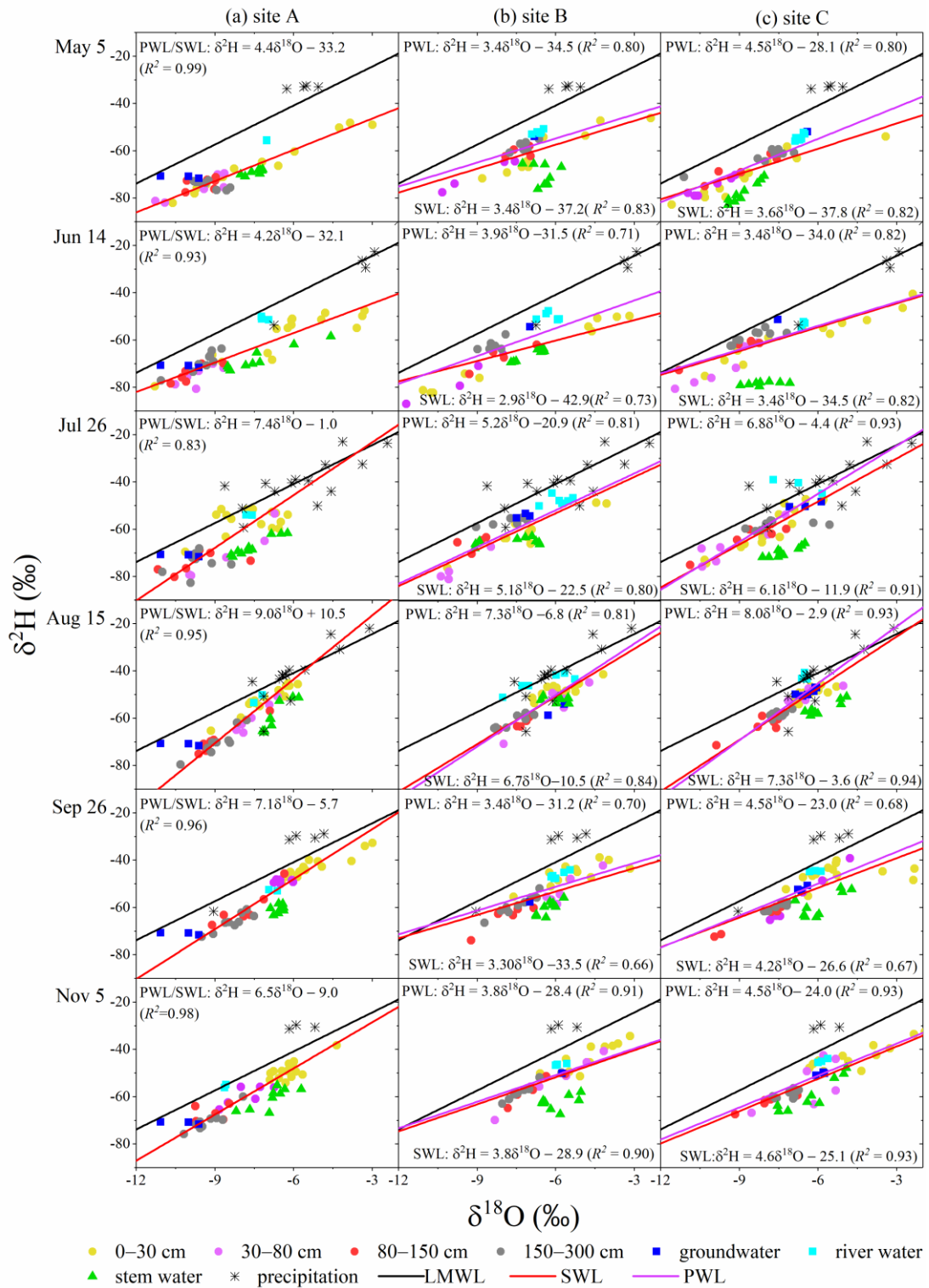


Fig. 5. Dual-isotopes ($\delta^2\text{H}$ and $\delta^{18}\text{O}$) plots of stem water of the riparian trees and their potential water sources (soil water in different layers, precipitation, groundwater, and river water) at sites (a) A, (b) B, and (c) C on six sampling campaigns during the observation period in 2019. The significant levels of all SWL and PWL are less than 0.001 ($p < 0.001$).

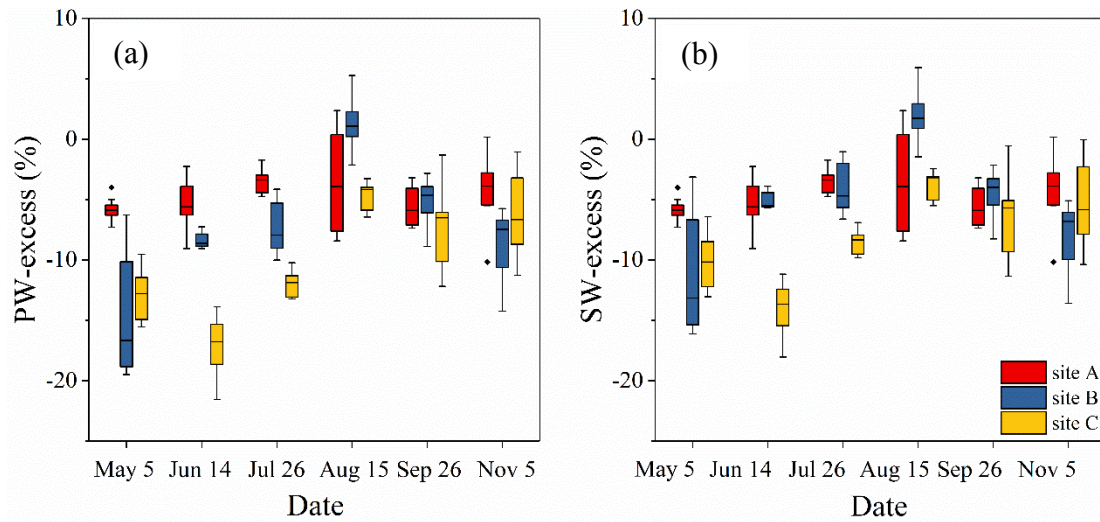


Fig. 6. Seasonal variations in the (a) PW-excess and (b) SW-excess of riparian trees at sites A, B, and C. The PW-excess value is as the same as the SW-excess value at site A. The box lines represent means and standard deviations (SD), whiskers indicate maximum and minimum values, and black diamonds are outliers.

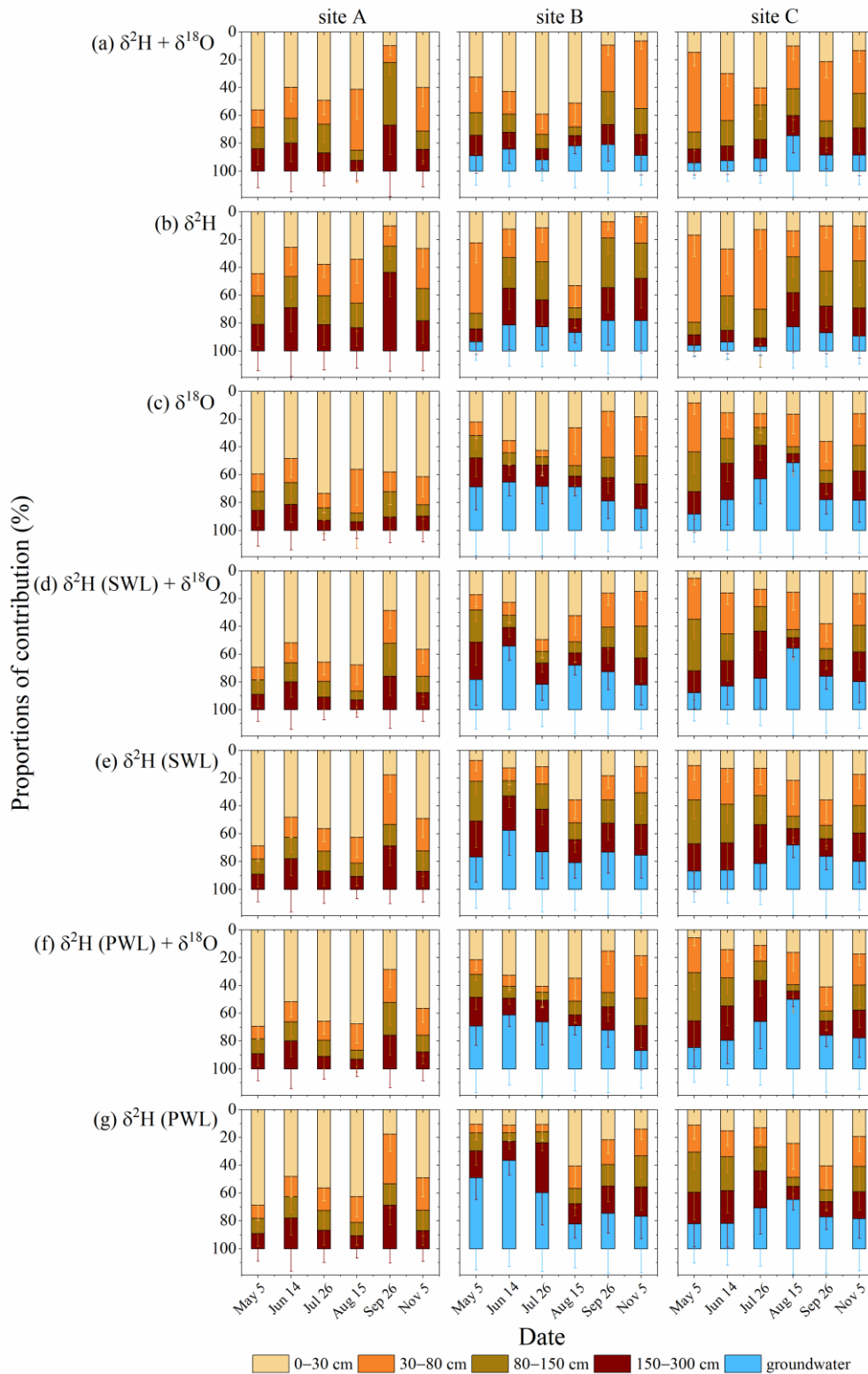


Fig. 7. Seasonal water uptake patterns for riparian trees at sites A, B, and C estimated via the MixSIAR model incorporating with (a) uncorrected $\delta^2\text{H}$ and $\delta^{18}\text{O}$, (b) uncorrected $\delta^2\text{H}$, (c) $\delta^{18}\text{O}$, (d) $\delta^2\text{H}$ corrected by SWL and $\delta^{18}\text{O}$, (e) $\delta^2\text{H}$ corrected by SWL, (f) $\delta^2\text{H}$ corrected by PWL and $\delta^{18}\text{O}$, and (g) $\delta^2\text{H}$ corrected by PWL. The MixSIAR model outputs using PWL correction method is same with those using SWL correction method at site A.

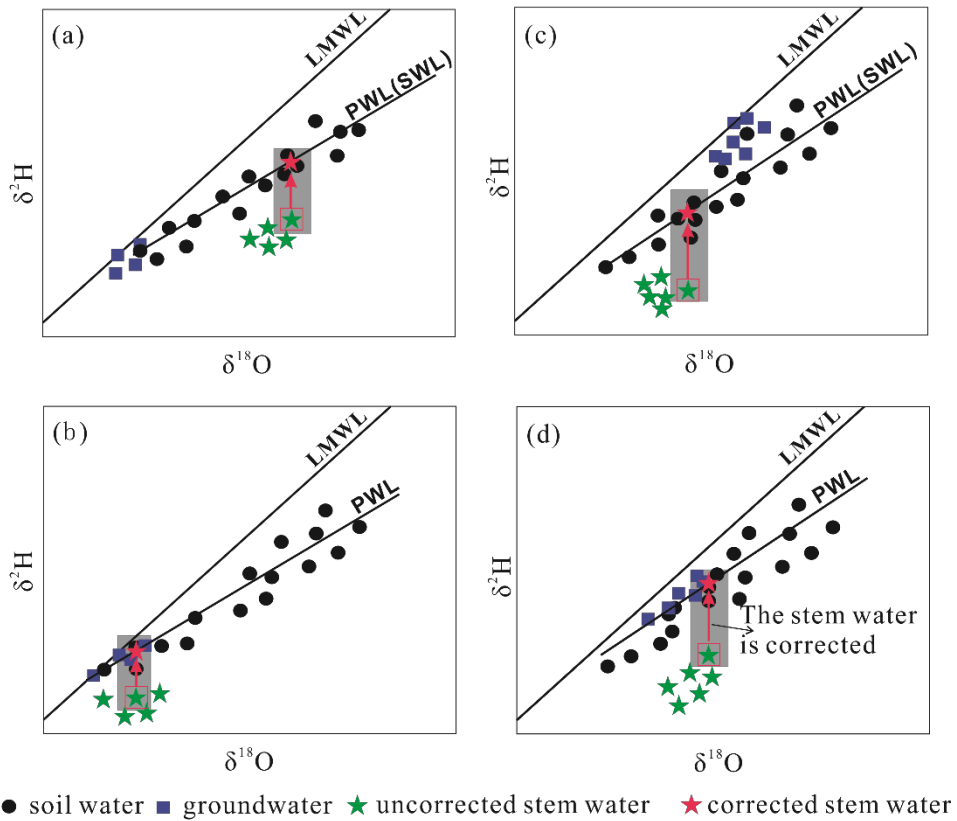


Fig. 8. Different types of $\delta^2\text{H}$ offset between stem water and its potential water sources shown in dual-isotopes ($\delta^2\text{H}$ and $\delta^{18}\text{O}$) plots. The potential water sources in the shaded area represent main water sources of the enclosed stem water sample by the red square. The red star represents the $\delta^2\text{H}$ -corrected stem water which derives from the enclosed stem water by the red square.

Supplementary material for on-line publication only

[Click here to download Supplementary material for on-line publication only: Table S1.docx](#)

Yue Li: Methodology; Formal analysis; Investigation; Writing - original draft; Writing - review & editing

Ying Ma: Conceptualization; Methodology; Formal analysis; Writing - review & editing

Xianfang Song: Supervision; Writing - review & editing; Project administration

Lixin Wang: Conceptualization; Writing - review & editing

Dongmei Han: Writing - review & editing